ISSN: 2321-2152

IJMECE

International Journal of modern electronics and communication engineering

E-Mail
editor.ijmece@gmail.com
editor@ijmece.com

www.ijmece.com

ISSN2321-2152www.ijmece .com

Vol 9, Issue 4 Dec 2021

Micropolar fluid flow across a stretched surface is affected by ohmic heating and chemical reactions

Mrs.M.Kavitha, Mrs.Lavanya Gullani, Mr.MD.Giasuddin

Abstract; The present paper examine the interaction between the Ohmic heating and chemical reaction influence on MHD micropolar fluid flow through a stretching surface in the presence of chemical reaction employing Runge–Kutta– Fehlberg technique (RKF-45) along with the shooting process. By performing various similarity transformations, the governing equations were transformed to ODEs. Numerical implications were computed for various values of important parameters on flow, rotational velocity, heat, mass transfer are presented visually and the numerical outcomes of the skin friction, couple stress at the wall, Nusselt number, Sherwood number are recorded in tabular form. With a rise in the material parameter, the velocity, couple stress, Sherwood number, Nusselt number, and temperature, concentration, and shear stress increase, while temperature, concentration, and shear stress falls

Introduction;Heat and mass transport analysis is crucial in many engineering and sciences. This topic has different applications in engineering such as petroleum reservoir, nuclear waste disposal, ground water hydrology etc., and because of this, it is crucially necessary to further explore non Newtonian fluids. The hypothesis of micropolar fluids was advocated by Eringen. 1 Micropolar fluids are extensively employed in the heat and mass transfer and boundary layer flow field. Several study papers were published in the literature on thermal boundary layer flows. Bakr2 anal ysed the MHD natural convection heat and mass transfer micropolar fluid using oscillating plate. G. Ahmadi,3 Rees and Pop4 examined th

micropolar fluid flow across a vertical plate. Mansour et al.5 discuss the MHD movement of micropolar fluid on the circular with heat and mass flux. MHD flow in a micropolar fluid with continuous suction had been considered by Amin. 6 Takhar et al.7 investigated Micropolar fluid mixed convection flow across a stretched sheet. Mansour et al.8 examined the thermal stratification influences on heat transfer flow of micropolar fluid owing to a stretched sheet with suction/injection. Many authors9–13 have researched the free and mixed convections of a micropolar fluid via a moving surface in different settings. For the free convective stratified fluid flow over an infinite vertical plate with Hall impact, BSGoud et al.14 looked at the numerical results. A moving vertical porous plate with suction and injection effects was used by HSNaik et al.15 to study free convective fluid flow. Considered by Eldabe et

1,2 Assistant Professor , Associate Professor
Department of H&S
Global Institute of Engineering and Technology,Moinabad,RR District, Telangana State

al.16,17 the hydromagnetic micropolar fluid flow of a previous stretching surface by Corresponding author. nandeppanavarmm@gmail.com is my email address (M.M. Nandeppanavar). The Chebyshev finite difference technique is being used. Mahmoud18 studied the MHD flow of a micropolar fluid across a stretched sheet with thermal conductivity and radiation effects. An MHD stagnation point was used by Hayat et al.19 to examine the micropolar fluid flow across a non-linear stretching surface. The stagnation flow of a micropolar fluid through a porous material was examined by Nadeem et al.20. Ishak21 describes the flow of a micropolar fluid through a thermally bonded ary layer with radiation impact across a stretched sheet. Thermal radiation and a curved stretching sheet were used by Naveed et al. to study micropolar fluid movement. 22 Rashidi et al. discussed the analytical approximation issue for the heat transport of a micropolar fluid across a porous media with the radiation effect. 23 With slip and boundary conditions, BSGOUD24 proved the MHD stagnation point flow. Micropolar fluid flow in a porous media with suction toward a stretching/shrinking sheet was studied by Rosali et al.25. Several writers also investigated various elements, such as 26–28. In the presence of a chemical reaction, the current work examines the effects of Ohmic heating and viscous dissipation on the MHD flow of micropolar fluid across a stretched sheet. The RKF-45 and firing process are used to solve the nonlinear ODEs. Graphs and tables show the effects of many important flow, angular velocity, temperature, and concentration parameters.

Nomenclature

υ	Kinematics viscosity
k	Vortex viscosity
γ	Viscosity of spin gradient.
ρ	Free stream density
T	Fluid temperature within the boundary layer
M	Magnetic parameter
u_w	Surface velocity
j	Microinertia per unit mass
C_w	Species concentration at the surface.
k_f	Thermal conductivity
Sc	Schmidt number
μ	Dynamic viscosity
C_p	Specific heat constant pressure
D	Coefficient of Mass diffusivity
b	constant
C	Fluid concentration within the boundary layer
Pr	Prandtl number
T_w	Surface temperature
T_∞	Fluid temperature far from the surface
C_∞	Fluid concentration far from the surface
K	Material parameter
Ec	Eckert number

Problem description

An electrically conducting fluid is a steady 2-D natural convection with heat and mass transfer micropolar flow caused by a moving surface within an incompressible fluid. It's assumed that you're going to choose the x-axis to be parallel with the sheet of paper, while the y-axis will be vertically aligned. The induced magnetic field is ignored when magnetic Reynolds numbers are assumed to be extremely tiny, and the magnetic field is employed in a route normal to the stretched sheet. Include the fascinated electric field and leave off the Hall effect as an additional option. It is assumed here that the fluids are homogeneous. The system is governed by the following equations [Ref. 16].

$$\frac{\partial u}{\partial x}+\frac{\partial v}{\partial y}=0 \tag{2.1}$$

$$u\frac{\partial u}{\partial x}+v\frac{\partial u}{\partial y}=\left(v+\frac{k}{\rho}\right)\frac{\partial^2 u}{\partial y^2}+\frac{k}{\rho}\frac{\partial N}{\partial y}-\frac{\sigma B_0^2}{\rho}u-\frac{v}{K_p}u \tag{2.2}$$

$$u\frac{\partial N}{\partial x}+v\frac{\partial N}{\partial y}=\frac{\gamma}{j\rho}\frac{\partial^2 N}{\partial y^2}-\frac{k}{j\rho}\left(2N+\frac{\partial u}{\partial y}\right) \tag{2.3}$$

$$u\frac{\partial T}{\partial x}+v\frac{\partial T}{\partial y}=\frac{k_f}{\rho c_p}\frac{\partial^2 T}{\partial y^2}+\frac{\mu+k}{\rho c_p}\left(\frac{\partial u}{\partial y}\right)^2+\frac{\sigma B_0^2}{\rho c_p}u^2 \tag{2.4}$$

$$u\frac{\partial C}{\partial x}+v\frac{\partial C}{\partial y}=D\frac{\partial^2 C}{\partial y^2}-k_o(C-C_\infty) \tag{2.5}$$

Along with the boundary conditions

$$\left.\begin{array}{ll} u=u_w=bx, v=0, N=0, T=T_\infty, C=C_\infty & : y=0 \\ u=0, N=0, T=T_\infty, C=C_\infty & : y\to\infty \end{array}\right\} \tag{2.6}$$

Eqs. (2.4) and (2.5) are examples of the R.H.S. of Eqs. (2.4) and Eqs (2.5). Ref. 4 is expected to give in this scenario. In order to verify that Eqs. (2.1–2.3) properly predict the precise behaviour when microstructure effects are minor, and the microrotation (N) is translated to the angular velocity, (2.4) is employed to ensure that j = b show the length of reference. 3 Coordinate transformation and dimensionless thermophysical parameter are introduced:

$$\left.\begin{array}{c} \eta=\sqrt{\frac{b}{v}}y, u=bxf'(\eta), v=-\sqrt{bv}f(\eta), M=\frac{\sigma B_0^2}{\rho b}, K=\frac{k}{\mu}, \\ N=\sqrt{\frac{b^3}{v}}xg(\eta), \\ \theta(\eta)=\frac{T-T_\infty}{T_w-T_\infty}, \phi(\eta)=\frac{C-C_\infty}{C_w-C_\infty}, Kp=\frac{bkp}{v}, \Pr=\frac{\rho v C_p}{kf}, \\ Ec=\frac{u_w^2}{C_p(T_w-T_\infty)}, \\ Sc=\frac{v}{D}, Kc=\frac{k_o}{b} \end{array}\right\}$$

Eq. (2.1) automatically satisfied and by employing the Eqs. (2.8) into Eqs. (2.1)–(2.6) changed to the following form:

$$(1+K)f'''+ff''+Kg'-(f')^2-\left(M+\frac{1}{Kp}\right)f'=0 \tag{2.9}$$

$$\left(1+\frac{K}{2}\right)g''+fg'-f'g-K(2g+f'')=0 \tag{2.10}$$

$$\theta''+Prf\theta'+(1+K)PrEcf''+PrEcMf'^2=0 \tag{2.11}$$

$$\phi''+Scf\phi'-ScKc\phi=0 \tag{2.12}$$

$$\left.\begin{array}{ll} f'=1, f=0, N=0, \theta=1, \phi=1 & : \eta=0 \\ f'=0, N=0, \theta=0, \phi=0 & : \eta\to\infty \end{array}\right\} \tag{2.13}$$

The shear stress is defined as

$$\tau_w=\left[(\mu+k)\left(\frac{\partial u}{\partial y}\right)+kN\right]_{y=0}=bx(\mu+k)\sqrt{\frac{b}{v}}f''(0) \tag{2.14}$$

The local skin friction factor C_f can be written as

$$C_f=\frac{\tau_w}{\rho U_w^2}=\frac{1+K}{\sqrt{Re_w}}f''(0) \tag{2.15}$$

At the wall surface, the couple stress is referred as

$$M_w=\gamma\left(\frac{\partial N}{\partial y}\right)_{y=0}=\mu u_w\left(1+\frac{K}{2}\right)g'(0) \tag{2.16}$$

The local Nusselt number, local surface heat flux, local mass flux, and Sherwood number is defined as

$$q_w(x)=-k_f\left(\frac{\partial T}{\partial y}\right)_{y=0}=-k_f(T_w-T_\infty)\sqrt{\frac{b}{v}}\theta'(0) \tag{2.17}$$

$$Nu_x=\frac{xh(x)}{k_f}=\frac{xq_w(x)}{k_f}=-\sqrt{\frac{b}{vx}}\theta'(0) \text{ on simplification } \frac{Nu_x}{\sqrt{Re_w}}=-\theta'(0) \tag{2.18}$$

The local mass flux can be defined as $j_w=-D\left(\frac{\partial C}{\partial y}\right)_{y=0}$, therefore the Sherwood number can be written as

$$Sh_x=\frac{j_x x}{D(C_w-C_\infty)}=-\sqrt{\frac{b}{vx}}\phi'(0) \text{ or } \frac{Sh_x}{\sqrt{Re_w}}=-\phi'(0) \tag{2.19}$$

Numerical process

The RKF-45 scheme and the shooting technique are used to solve the set of ODEs (2.9)–(2.12) and the limits (2.13) numerically. To find a solution, go through the procedures listed below: • BVP becomes IVP. Initial estimate values are taken at random, and the Secant technique is used to acquire a more accurate answer for these evaluations by using the Secant method.

Ref. 16 and the current investigation are compared in Table 1 based on various values of P r = 0.71, K = 0 Ec = 0.02, Sc = 0.2, and absence of the Kc, Kc

M	Eldabe et al.[16] $-f''(0)$	Present study $-f''(0)$	*error*
0	1.000008368810236	1.0000080397275981	3.2908×10^{-7}
0.5	1.224744915271371	1.2247453246251598	4.0935×10^{-7}
1	1.4142135628866208	1.4142139165176042	3.5363×10^{-7}
3	1.9999999999427769	2.0000002500032092	2.5006×10^{-7}

In order to calculate IVP, the RKF-45 scheme with a step difference of 0.001 should be employed, with h = 0.001. The selected convergent precision of 106 outcomes of order required a large number of RKF-45 iterations. In order to determine the best step size (h), this technique comprises a method. Two new approximations are generated and compared at each stage. The step size is adjusted based on the results so that the estimations are as close as possible to each other. Using RK-fourth order methods, the answer to the problem is found.

$$y_{m+1} = y_m + \frac{25}{216}k_1 + \frac{1408}{2565}K_3 + \frac{2197}{4104}k_4 - \frac{1}{5}k_5$$

A better solution is found using a RK scheme of order 5.

$$y_{m+1} = y_m + \frac{16}{135}k_1 + \frac{6656}{12825}K_2 + \frac{28561}{56430}k_4 - \frac{9}{50}k_5 + \frac{2}{25}k_6$$

Each step necessitates the application of the six values listed below:

$$k_1 = hf(z_k, t_k)$$

$$k_2 = hf\left(z_k + \frac{h}{4}, t_k + \frac{k_1}{4}\right)$$

$$k_3 = hf\left(z_k + \frac{3h}{8}, t_k + \frac{3}{32}k_1 + \frac{9}{32}k_2\right)$$

$$k_4 = hf\left(z_k + \frac{12h}{13}, t_k + \frac{1932}{2197}k_1 - \frac{7200}{2197}k_2 + \frac{7296}{2197}k_3\right)$$

$$k_5 = hf\left(z_k + h, t_k + \frac{439}{216}k_1 - 8k_2 + \frac{3680}{513}k_3 - \frac{845}{4104}k_4\right)$$

$$k_6 = hf\left(z_k + \frac{h}{2}, t_k - \frac{8}{27}k_1 + 2k_2 - \frac{3544}{2565}k_3 - \frac{1859}{4104}k_4 - \frac{11}{40}k_5\right) \quad (3.20)$$

By combining the above mentioned procedures with the shooting technique, numerical solutions obtained with accuracy 10−6 of the present problem.

Results and discussion

The RKF-45 and firing approach are used to solve the ODEs (2.9)–(2.12) with constraints (2.13) in the given set. Numbers are calculated according to problem constraints and then tabulated and displayed with graphical illustrations to help gain a physical understanding of flow, temperature, and concentration distribution. This is illustrated in Figures 1–4 for different magnetic parameter (M) values: nondimensional velocity (f ′) curves, temperature curves, concentration curves, and angular velocity (g). The Lorentz force opposes the flow, so an increase in M reduces velocity and angular velocity; however, the Ohmic heating effect has the opposite effect, increasing temperature and concentration. Material parameter (K) behaviour on velocity, angle of velocity, concentration and temperature distribution is shown graphically in Figures 5–8. The f′ and g values rise as the K mean increases, whereas the and values fall. The angular velocity of the additive increases as the viscosity of the fluid decreases. In Fig. 9, the temperature curves for various values of the Prandtl number (P r) are shown. Temperature distribution is reduced as a consequence of increasing the values of P r (beginning with air 0.71). This is as a result of the fact that

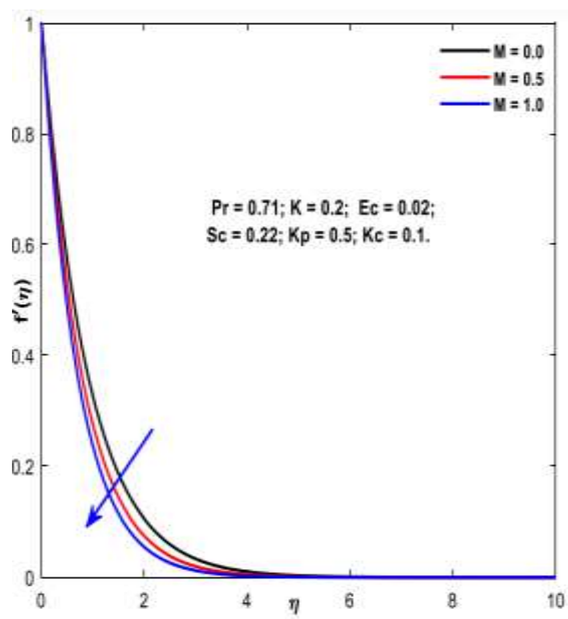

Fig. 1. *M* v/s Velocity

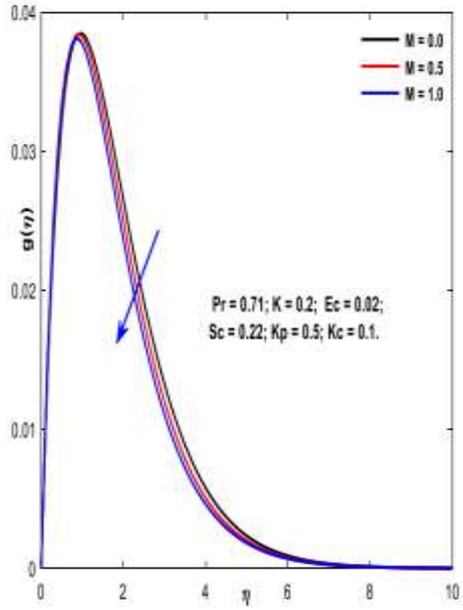

Fig. 2. M v/s Angular velocity.

When Pr increases the thickness of the thermal boundary layer diminutions. Eckert number(Ec) behaviour on the temperature distribution is depicted in Fig. 10. It is discovered that boosting Ec is to raise the temperature in the boundary layer. The behaviour of the Schmidt number on the concentration curves is depicted in Fig. 11. For taking the increasing values of ($H2$ = 0.22, $H2O$ = 0.6, $NH3$ = 0.78, $CO2$ = 0.94) the results in concentration declines. Figs. 12–15 demonstrate the behaviour of the permeability parameter (Kp) on the velocity, angular velocity and temperature & concentration. As raising the Kp value the outcomes in $f\ '$ and g curves are enhanced, reverse observations can be noticed in θ and ϕ declines. The concentration profile are presented in Fig. 16 for various numbers of chemical reaction parameter (Kc). It is apparent that presence of Kc is to lower the concentration dispersion. This is reason why the Solutal boundary layer falls with Kc. Table 1 displays the comparison between the Chebyshev finite difference technique and RKF-45 approach. The implications of the shear stress produced via the Chebyshev finite difference approach are in excellent agreement with the results derived from the RKF-45 technique, as shown in Table 1. The fluctuation of $-f''(0)$, $g'(0)$, $-\theta'(0)$, and $-\phi'(0)$ for the influence of the M&K is given in Tables 2 and 5.

Table 2 Comparison with Eldabe et al.16 for multiple values of the $-f''(0)$, $g'(0)$, $-\theta'(0)$, and $-\phi'(0)$ for varied values of M and K with Ec = 0.02, Pr = 0.71, Sc = 0.2, absence of Kp and Kc.

M	K	Present study			
		$-f''(0)$	$g'(0)$	$-\theta'(0)$	$-\phi'(0)$
0.0	0.2	[illegible]	[illegible]	[illegible]	[illegible]
0.5	0.2	[illegible]	[illegible]	[illegible]	[illegible]
1.0	0.2	[illegible]	[illegible]	[illegible]	[illegible]
1.0	0.0	[illegible]	[illegible]	[illegible]	[illegible]
1.0	0.5	[illegible]	[illegible]	[illegible]	[illegible]
1.0	2.0	[illegible]	[illegible]	[illegible]	[illegible]

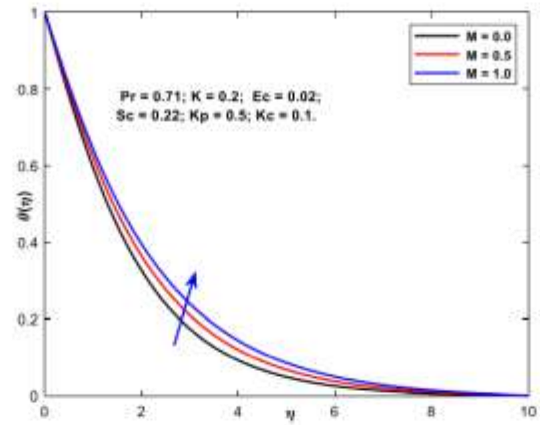

Fig. 3. M. v/s Temperature.

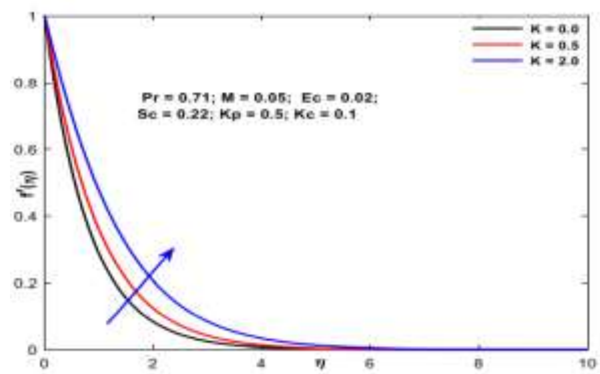

Fig. 5. Velocity v/s K.

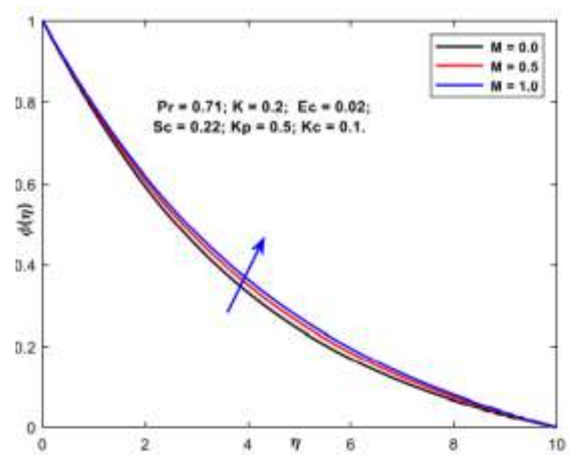

Fig. 4. Concentration v/s M.

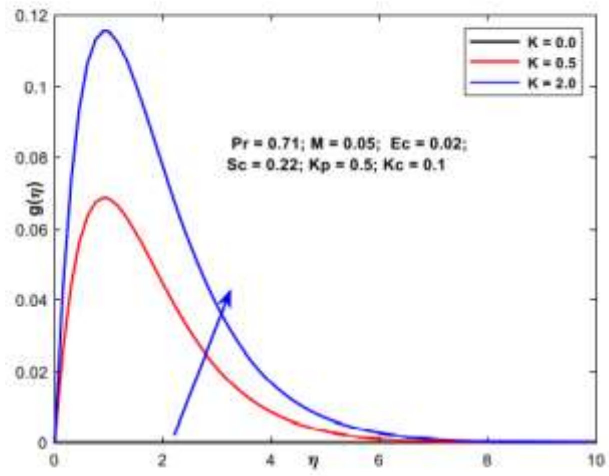

Fig. 6. *K* v/s Angular velocity

An increase in the values of M results in an increase in the values of (g) and (f), while the opposite is seen in (g) and (f) when the values of M are increased (0). There is an accompanying rise in K-values that affects all of these variables, as well as an associated decrease in K-values that affects all of these variables. The existence or absence of Kp and Kc also allows for comparison. Tables 3 and 6 show the ′ (0) with different values of P r when Kp and Kc are present or absent. The table shows that ′ (0) rises with an increase in P r. In Table 4, you can see how various values of Sc affect the influence of ′ (0). In the absence of Kc and Kp, a rise in Sc results in an increase in ′ (0). Sc and Kc's effect on ′ (0) is seen in the figure.The values of P r and Ec, as well as M, as well as K, Sc, and Kp, are all set to one; the results of these calculations are shown in Table 3.

Pr	Eldabe et al.[16] $-\theta'(0)$	Present study $-\theta'(0)$
0.71	0.3913495637393539	0.4159216373670690
1	0.5035077972221575	0.5369521756305649
2	0.8106974076252109	0.8718439515257624

Conclusions

Numerical analysis is utilised in the current work to assess the influence of the Ohmic heating and chemical reaction parameter on MHD micropolar fluid, through a stretching surface in the occurrence of the porous medium A similarity change was used to convert the flow equations into ODEs. The RKF 45 technique may be used to solve these equations. The following pertinent factors have shown interesting visual results: M increases shear stress, Nusselt number, and Sherwood number while decreasing velocity, Nusselt number, and Sherwood number. There is a decrease in shear stress when the material parameter is raised, but the Sherwood and Nusselt numbers rise. Temperature falls and - ′ (0) rises with an increase in P r values. • A drop in concentration and an increase in ′ (0) are both caused by an increase in Sc and Kc.

References

1. Eringen AC. Theory of micropolar fluids. J Math Anal Appl. 1972;38:469–480.

2. Bakr AA. Effects of chemical reaction on MHD free convection and mass transfer flow of a micropolar fluid with oscillatory plate velocity and constant heat source in a rotating frame of reference. Commun Nonlinear Sci Numer Simul. 2011;16(2):698–710.

3. Ahmadi G. Self-similar solution of incompressible micropolar boundary layer flow over a semi-infinite flat plate. Internat J Engrg Sci. 1976;14:639–646.

4. Rees DAS, Pop I. Free convection boundary layer flow of a micropolar fluid from a vertical flat plate. IMA J Appl Math. 1998;61:179–197.

5. Mansour MA, El-Hakiem MA, El Kabeir SM. Heat and mass transfer in magnetohydrodynamic flow of micropolar fluid on a circular cylinder with uniform heat and mass flux. J MagnMagn Mater. 2000;220(2–3):259–270.

6. El-Amin MF. Magnetohydrodynamic free convection and mass transfer flow in micropolar fluid with constant suction. J MagnMagn Mater. 2001;234(3):567–574.

7. Takhar H, Agarwal R, Bhargava R, Jain S. Mixed convection flow of a micropolar fluid over a stretching sheet. Heat Mass Transf. 1998;34:213–219. http://dx.doi.org/10.1007/s002310050252, 1998.

8. Mansour MA, Mohamed RA, Abd-Elaziz MM, Ahmed SE. Thermal stratification and suction/injection effects on flow and heat transfer of micropolar fluid due to stretching cylinder. Int J Numer Methods Biomed Eng. 2011;27:1951–1963. http://dx.doi.org/10.1002/cnm.1449.

9. Agarwal RS, Bhargava Rama, Balaji AVS. Finite element solution of flow and heat transfer of a micropolar fluid over a stretching sheet. Internat J Engrg Sci. 1989;27(11):1421–1428. http://dx.doi.org/10.1016/0020-7225(89)90065-7.

10. Abo-Eldahab Emad M, Ghonaim Ahmed F. Radiation effect on heat transfer of a micropolar fluid through a porous medium. Appl Math Comput. 2005;169(1):500–510. http://dx.doi.org/10.1016/j.amc.2004.09.059.

11. Bejawada Shankar Goud, Khan Zafar Hayat, Hamid Muhammad. Heat generation/absorption on MHD flow of a micropolar fluid over a heated stretching surface in the presence of the boundary parameter. Heat Transfer. 2021;50(6):6129–6147. http://dx.doi.org/10.1002/htj.22165.

12. Shankar Goud B. Heat Generation/Absorption influence on steady stretched permeable surface on MHD flow of a micropolar fluid through a porous medium in the presence of variable suction/injection. Int J Thermofluids. 2020;7–8:100044. http://dx.doi.org/10.1016/j.ijft.2020.100044. 13. Rahman MM, *Sattar MA. Transient convective flow of micropolar fluid past a continuously moving vertical porous plate in the presence of radiation. Int J Appl Mech Eng. 2007;12:497–513.*

14. Shankar Goud B, Sudhakar Reddy K, Suresh P, Ramana Murthy MV. Numerical solution of free convective stratified fluid flow over an infinite vertical porous plate with hall effect. Int J Mech Prod Eng Res Dev. 2020;10(3):10019–10030.

15. Naik Hari Singh, Shankar Goud B, Suresh P, Ramana Murthy MV. Suction/injection effects on free convective fluid flow over a moving vertical porous plate with variable time. J Crit Rev. 2020;7(18):1324–1328.

16. Eldabe NT, Ouaf Mahmoud EM. Chebyshev finite difference method for heat and mass transfer in a hydromagnetic flow of a micropolar fluid past a stretching surface with Ohmic heating and viscous dissipation. Appl Math Comput. 2006;177:561–571.

17. Eldabe NT, Elshehawey EF, Elsayed, Elbarbary ME, Elgazery Nasser S. Chebyshev finite difference method for MHD flow of a micropolar fluid past a stretching sheet with heat transfer. Appl Math Comput. 2005;160(2):437–450. http://dx.doi.org/10.1016/j.amc.2003.11.013.

18. Mahmoud Mostafa AA. Thermal radiation effects on MHD flow of a micropolar fluid over a stretching surface with variable thermal conductivity. Physica A. 2007;375(2):401–410.

19. Hayat T, Javed T, Abbas Z. MHD flow of a micropolar fluid near a stagnationpoint towards a non-linear stretching surface. Non-Linear Anal: Real World Appl. 2009;10:1514–1526.

20. Nadeem S, Hussain M, Naz M. MHD stagnation flow of a micropolar fluid through a porous medium. Meccanica. 2010;45:869–880. http://dx.doi.org/10. 1007/s11012-010-9297-9, 2010.